Interaction of clinical-stage antibodies with heme predicts physiochemical and functional liabilities relevant for developability

Maxime Lecerf[1], Alexia Kanyavuz[1], Sofia Rossini[1], and Jordan D. Dimitrov[1*]

[1]Centre de Recherche des Cordeliers, INSERM, Sorbonne Université, Université de Paris, F-75006 Paris, France

*Corresponding author: Jordan D. Dimitrov

E-mail: jordan.dimitrov@sorbonne-universite.fr / jordan.dimitrov@inserm.fr

Running title: Interaction of clinical-stage antibodies with heme

Keywords: therapeutic antibodies; antibody developability; analytical tools; heme; antibody polyreactivity; physicochemical properties of antibodies.

Abstract

Development of monoclonal antibody therapeutics is a sophisticated process. Early stage detection of negative traits of antibodies, which can impact the production, storage stability or therapeutic efficacy is of critical importance for saving time and resources in drug development programs. Since the developability issues of antibodies are diverse, including expression yield, chemical and physical stability, propensity for aggregation, antigen-binding polyreactivity, etc., a battery of experimental and *in silico* assays have been developed for thorough examination of drug candidates. Here, by using a set of 113 samples with variable region sequences matching clinical-stage therapeutic antibodies, we demonstrated that unique physicochemical properties of heme allow this cofactor molecule to be applied as a probe for simultaneous detection of different deleterious characteristics of antibodies *i.e.*, antigen-binding polyreactivity, self-association, aggregation, hydrophobicity and expression yield. Moreover, our study demonstrates that similarly as antibody repertoires from healthy individuals, a fraction of therapeutic antibodies acquires use heme as cofactor for recognition of diverse antigens. These results reveal presence of a hidden vulnerability issue for some antibodies, which would not be detectable by standard analytical assays. This liability may be of concern for monoclonal antibodies intended to be use in patients with pathophysiological conditions where extracellular heme is present *e.g.* hemolysis or tissue damage. We provided evidence about the mechanistic basis of the unique features of heme and offer a powerful analytical tool for rapid and simple detection of important negative traits in candidate therapeutic antibodies.

Introduction

Use of monoclonal therapeutic antibodies (Abs) for treatment of human diseases represents an important milestone of modern medicine. Presently, approximately 90 therapeutic Abs are successfully applied for treatment of cancer, autoimmune, inflammatory and infectious diseases (1,2). Hundreds of other Ab molecules are in clinical trials or are under development. The principal operational mechanism of therapeutic Abs is based on a high-fidelity recognition of a specific disease-associated target, followed by its inhibition or by induction of secondary immune reactions through the constant immunoglobulin fragment. To become a successful therapeutic, however, mere identification of an Ab molecule with high binding affinity to a specific target of interest is often not sufficient. Indeed, high affinity recognition of antigen can be accompanied with various additional features of the immunoglobulin molecule that can have a negative impact on the production process, pharmacokinetics and ultimate therapeutic efficacy. These features include expression yield, thermodynamic stability, propensity for aggregation, sensitivity to chemical degradation, immunogenicity, antigen-binding polyreactivity and self-binding capacity (3-6). Each of these variables might have negative economical and clinical impact on production and use of the therapeutic Abs. For example, elevated tendency for aggregation and/or self-binding would compromise the use of antibody at high concentrations; low chemical and thermodynamic stability would reduce shelf life; the potential for binding to many dissimilar antigens *i.e.* antibody polyreactivity, would strongly impact the Ab pharmacokinetics, resulting in a faster *in vivo* clearance, etc.

The process of development of therapeutic monoclonal Abs is sophisticated, resource- and time-consuming (7). Therefore, use of simple predictive tools that can detect at early stage different developability issues is of high importance. Many approaches have been developed for *in vitro* or *in silico* evaluation of the various physicochemical features of Abs that can allow recognition of those with developability problems (6,8-16). From these studies it is evident that only the simultaneous use of complementary analytical techniques would allow comprehensive interrogation of all possible developability issues of a particular Ab. In the study of Jain et al (17), comprehensive analyses of 137 therapeutic Abs with an array of 12 complementary assays demonstrated the advantage of an integrative approach for successful identification of Abs with unfavourable biophysical and functional characteristics. Importantly, the statistical analyses in this study revealed marked interrelation between various biophysical qualities of Abs.

Besides developability traits that are constantly present in Abs, some unfavourable characteristics can be cryptic and thus become apparent only after exposure of Ab molecule to certain conditions. Thus, in addition to intrinsically polyreactive Abs that express their antigen-binding promiscuity constantly (18,19), a fraction of human Abs can acquire potent polyreactive behaviour post-translationally upon *in vitro* or *in vivo* exposure to redox-active substances, including the physiologically-relevant cofactor heme (20-24). Notably, by analyses of a set of 9 therapeutic Abs approved for treatment of cancer, it was demonstrated that after exposure to heme most of the Abs acquired substantial polyreactivity (25). Since the pharmacological stability of Ab may be compromised *in vivo* upon potential exposure of the Ab to heme (or other redox active substances), identification of hidden developability issues is of utmost importance.

Here we assessed the use of interaction of Abs with heme as a novel indicator for therapeutic Ab developability. The obtained results clearly highlight the importance of the hidden developability issues in analyses of human therapeutic Abs. More importantly, our results obtained with 113 samples with V region sequences corresponding to clinical-stage therapeutic monoclonal Abs also revealed that interaction with heme can be used as a potent integrative predictive hallmark for number of developability problems that are usually detected by several independent techniques; *e.g.*, Ab hydrophobicity, expression yield, natural polyreactivity, self-binding and cross-reactivity to other immunoglobulins. Thus, we provide strong evidence for utility of heme as a molecular probe for parallel detection of several problematic features of candidate therapeutic Abs.

Results

Interaction of therapeutic Abs with heme

Interaction of certain human Abs with biological cofactor molecule heme (Fe-protoporphyrin IX, Fig. 1A) can result in appearance antigen-binding polyreactivity (21). Since heme is abundant *in vivo* and can be released extracellularly in many pathological conditions (26), we hypothesized that binding of Abs to heme can represent an important hidden developability issue for assessment of therapeutic Abs. In this study, we used a set of 113 monoclonal therapeutic Abs all expressed as human IgG1. At present, 44 of those Abs are approved for clinical use, and rest of the molecules are in Phase II and III clinical trials (except one – vesencumab).

First, to assess the binding of Abs to heme, we used a method based on immune sorbent assay, where heme is covalently attached to pre-coated carrier protein. The obtained results clearly demonstrate that a significant portion of Abs bind to immobilized heme (14 % of Abs binding with 10-fold higher intensity to immobilized heme as compared to carrier alone) (Fig. 1B). Next, the interaction of the therapeutic Abs set with another aromatic cofactor molecule, folic acid (FA), was evaluated. Number of Abs binding to surface-immobilized FA was lower as compared to heme-binding Abs (Fig. 1B). Nevertheless, Spearman's correlation analyses demonstrated a significant correlation between the reactivities of Abs against both heterocyclic cofactors ($\rho = 0.69$, $P < 0.0001$). The Abs that recognized heme with the highest intensity were subjected to additional analysis. Figure 1C depicts the Ab-concentration dependent binding to immobilized heme. Data indicates that those Abs bind with high avidity to heme (50 % of the maximal binding for most of the Abs was achieved by < 100 nM of IgG1). Two Abs (figitumumab and fulranumab) recognized surface-immobilized heme with *ca*. 10-fold higher avidity as compared to other Abs. In addition to the approach based on surface immobilization of heme, we studied the interaction of heme with Abs in solution by high-throughput UV-vis absorbance spectroscopy, and by determination of heme binding to Abs by examining the changes in the catalytic activity of heme (Fig. 2). These techniques confirmed that a fraction from the panel of therapeutic monoclonal Abs is capable of binding to heme. To determine the binding affinity of Abs to soluble heme, we used surface plasmon resonance-based technology. The obtained real-time interaction data of binding of heme to surface immobilized monoclonal Abs characterized an interaction with K_D values in the range of 313-509 nM (Fig. 1D). Furthermore, we applied

computational Ab modelling (Rosetta algorithm) to generate the most probable structural configuration of the antigen-binding site of a heme-binding Ab. The selected Ab (sample corresponding to the sequences of tigatuzumab) displayed the highest sensitivity to heme in terms of both binding and acquisition of polyreactivity (see Fig. 3A). By using ligand docking, structural model of variable region was used for prediction of the putative binding site for heme. As can be seen on Figure 1E, the binding site for heme is overlapping with the central part of antigen-binding region. This model suggests that heme molecule could establish interaction with CDR loops of both light and heavy immunoglobulin chains.

Acquisition of antigen-binding polyreactivity after interaction of therapeutic Abs with heme

To analyse whether the exposure to heme affects the antigen-binding properties of Abs, we next investigated the interaction of the panel of therapeutic Abs with a panel of unrelated proteins – human Factor VIII, human C3 and LysM domains of AtlA from *Enterococcus faecalis*. The binding of all Abs to immobilized proteins was assessed before and after the exposure to heme. Figure 3A illustrates that in their native state some of the therapeutic Abs have capacity to recognize the studied proteins. These Abs displayed natural antigen-binding polyreactivity since none of the studied proteins is cognate antigen of the studied therapeutic Abs. The obtained results also demonstrated that a fraction of therapeutic Abs acquired capacity to recognize the proteins only following contact with heme (Fig. 3A). The binding of heme-treated Ab to a given protein strongly correlated with binding to the other two proteins and to average binding reactivity against the three proteins (Fig. 3B). This result implies that the heme-sensitive Abs acquired antigen-binding polyreactivity upon exposure to heme. The Abs that demonstrated the highest gain in reactivity, as assessed by ELISA, were further subjected to immunoblot analyses. The observed recognition of multiple proteins from bacterial lysate confirmed the ability of heme to transform the binding behaviour of certain Abs (Fig. 3C). Previous works suggested that heme endows Abs with polyreactivity by binding to the antigen-binding site and serving as interfacial promiscuous cofactor facilitating contact with unrelated proteins (21). The docking analyses of the Ab displaying highest sensitivity to heme (Fig. 1E) are in full accordance with these findings.

Heme influenced selectively only Fab-dependent functions of Abs. Thus, SPR-based analyses revealed that the binding of native and heme-exposed Abs to human neonatal Fc receptor (FcRn) was characterized with no significant differences in the binding affinity (Fig. 4).

Sequence characteristics of antigen-binding site of Abs interacting with heme

To provide understanding about the molecular features of Abs responsible for interaction with heme and FA as well as acquisition of binding polyreactivity, we elucidated sequence characteristics of antigen-binding site of 113 Abs that overlap with molecules previously described in (17). We focused our analyses on the most diverse regions of the antigen-binding site *i.e.* CDR3 of heavy and light chains, as well as CDR2 of heavy chain, since the latter is the second most diverse region in antigen-binding site after CDRH3 and represents the second largest molecular surface for contact with antigens (27). By applying Spearman correlation analyses, it was observed that the length of CDRH3, CDRH2 and CDRL3 did not correlate with binding to heme and FA or with heme-induced polyreactivity (Fig. 5). No significant correlation was observed with the number of somatic mutations in the V regions either.

The analysis of frequencies of amino acid residues in CDRs revealed a number of statistically significant correlations. Thus, the ability of Abs to recognize heme positively correlated with the presence of a higher number of basic amino acid residues in CDRH3, particularly with the higher number of Lys (Fig. 5). Positive correlation of binding to heme was also observed for the numbers of Arg residues in CDRH2. This analysis also showed that both heme- and FA-binding Abs had a significantly lower frequency of acidic residues (Asp and Glu) in CDRH2. The heme-binding Abs have significantly higher number of Tyr residues in CDRH3. Frequency of another aromatic residue – Phe in CDRH3 and CDRH2

negatively correlated with higher binding to immobilized heme and FA. Interestingly, no statistically significant correlation was observed between frequency of any amino acid residue type in CDRL3 and the binding to heme or FA.

Next, we investigated the correlation of the heme-mediated acquisition of polyreactivity and sequence features of the antigen-binding site of Abs. The cryptic polyreactivity of the therapeutic Abs uncovered by heme negatively correlated with the presence of acidic residues in CDRH3. Similarly, as in the case of binding to heme, the Abs that acquired polyreactivity had significantly higher number of Tyr residues in CDRH3. Heme-sensitive Abs also presented an elevated frequency of Tyr in CDRH2. Abs acquiring polyreactivity following exposure to heme were characterized with lower frequencies of Ala and Leu in CDRH2 and CDRH3. Structural models of the selected Abs with the most pronounced heme-binding capacity and/or heme-induced polyreactivity revealed that positive charges and Tyr residues are well displayed on the molecular surface of the antigen-binding site (Fig. 6). The surface accessibility of positively charged amino acid residues and Tyr on the molecular surface of antigen-binding sites and their increased frequency suggest that these residues might play a direct role in interaction with heme.

Biophysical properties of the therapeutic Abs that interact with heme

In a previous study, Jain and colleagues quantified different physicochemical properties of a repertoire of 137 monoclonal therapeutic Abs (17). The measured features of Abs are of importance for developability and include – expression yield in HEK cells (HEKt), thermodynamic stability (Tm), accelerated stability (AS), tendency for self-association (ACSINS and CSI), binding to polyclonal human IgG (CIC), antigen-binding polyreactivity (PSR, ELISA, BVP) and hydrophobicity (SGAC100, HIC, SMAC). The panel of therapeutic Abs used in the present study overlaps with the repertoire of Abs that was used in the work of Jain (113 of the studied monoclonal Abs correspond to identical samples). This allowed us to analyse relationships between the physicochemical properties of the Abs assessed by different analytical techniques with their capacity to bind to heme or acquire polyreactivity upon exposure to heme. Statistical analyses revealed that the potential of therapeutic Abs to recognize immobilized heme strongly correlated with several biophysical properties of Abs that are of importance for developability assessment (Fig. 7). Thus, heme-binding Abs were characterized with significantly higher natural polyreactivity, as assessed by three independent polyreactivity assays (PSR, ELISA and BVP) (Fig. 7). Moreover, the increased binding to immobilized heme positively correlated with the tendency of the therapeutic Abs for self-binding and binding to other IgG molecules (ACSINS, CSI and CIC assays) (Fig. 7). These analyses revealed that the heme-binding Abs are generally aggregating at lower concentration of ammonium sulphate, *i.e.* they are characterized by elevated propensity for aggregation mediated by hydrophobic interactions (SGAC100 assay, Fig. 7). Interestingly, stronger association of heme had significant negative correlation with expression titer of the therapeutic Abs.

Further, we investigated the relationship of biophysical properties of the Abs with heme-induced polyreactivity. The heme-sensitive Abs had significantly higher overall hydrophobicity, as determined by three independent assays (SGAC100, HIC and SMAC). The Abs acquiring polyreactivity following contact with heme were also characterized by their intrinsic propensity for self-binding and cross-reactivity to human polyclonal IgG (Fig. 7).

Statistical analyses of results from different assays involving heme additionally suggested that heme-induced polyreactivity positively correlates with heme binding in solution and increase in ABTS oxidation (catalytic assay) (Fig. 7). Moreover, these analyses demonstrate that the study of Ab binding to immobilized heme or FA- and heme-induced Ab polyreactivity has considerably higher power in predicting developability issues of Abs as compared with the heme-binding assays in solution (absorbance spectroscopy and ABTS oxidation).

Clinical status of the heme-binding Abs

The studied panel of samples sourced V region sequences from therapeutic Abs molecules that

have been already approved for clinical use or are in phase II and phase III clinical trials. In previous work, it was shown that the Abs that entered clinical practice tend to be characterized by significantly lower number of developability problems as compared with Abs that had merely reached clinical trials (17). The threshold value of measures defining negative developability traits was set as the worst 10 % of value from different assays. By selecting Abs that bind heme with 10 % highest intensity (11 Abs in total), we found that among these Abs only two molecules have been approved for the clinical use (*i.e.* 18 %). Among the therapeutic Abs that bind less or do not bind at all to heme, 41 % have been approved for use in clinic. Most of the Abs (9 out of 11) showing the highest heme-binding intensity crossed at least one of the negative thresholds set for other developability assays in the study by Jain et al (17). Although the differences are not statistically significant due to low number of Abs, this result suggests that the interaction with heme is an indicator for the presence of developability issues of monoclonal Abs that might affect the final approval for clinical use.

Discussion

In the present study, we demonstrated that a considerable fraction of therapeutic Abs intended for clinical use recognizes heme. Moreover, exposure of some of the Abs to heme resulted in acquisition of antigen-binding promiscuity. We identified sequence patterns of the antigen-binding site that are associated with the interaction with heme and the induction of polyreactivity. Notably, the interaction with heme strongly correlated with three different groups of negative issues for Ab developability *i.e.* hydrophobicity, self-association and intrinsic polyreactivity, suggesting that this cofactor molecule has good potential as an integral probe for interrogation and detection of detrimental traits of Ab drug candidates.

Previous studies demonstrated that the immunoglobulin repertoires from healthy human donors have a fraction of Abs that acquire polyreactivity after exposure to heme. Thus, the interaction of heme with Abs results in appearance of high-affinity binding to autoantigens and pathogen-derived antigens (21,24,28). The frequency of Abs that change their binding behaviour after contact with heme was estimated to be 10-20 % depending on the studied antigen (24,29). Although the post-translational diversification of the antigen-binding specificity mediated by heme can have contribution to immune defense and immune regulation (24,29-31), this phenomenon would be highly undesirable for the therapeutic Abs. The appearance of polyreactivity can decrease potency and represents a risk for side effects due to compromised pharmacokinetics and off-target binding (6,9,32). By analysing a panel of clinical-stage therapeutic Abs, we demonstrated that this panel contains heme-sensitive Abs. In the current study, we analysed the monoclonal Abs for both heme binding and heme-induced antigen-binding polyreactivity. Interestingly, the correlation between the both parameters was significant but not very strong ($\rho = 0.359$; $P < 0.0001$). There were many Abs that bind to heme but did not acquire antigen-binding promiscuity and vice versa. This result can be explained by the fact that for the acquisition of polyreactivity, the heme molecule should be displayed in an appropriate manner on the antigen-binding site and most probably to be itself engaged in interactions with antigen (33). If heme binding results in burial of the macrocyclic molecule in the protein interior, this most probably would not cause acquisition of binding polyreactivity. Notably, the structural model of heme binding to the variable region of a monoclonal Ab that showed the most pronounced polyreactivity upon heme binding, tigatuzumab, suggested that the one of the molecular planes of heme is well exposed on the surface of antigen-binding site (Fig. 1E), and hence it can be involved in other interactions.

The elucidation of sequence characteristics of the variable region of Abs that bind to heme revealed positive correlation of the recognition of heme with the presence of Tyr residues in the most diverse region of the immunoglobulin molecule *i.e.*, CDRH3. The number of Tyr was also significantly elevated in the CDRH3 and CDRH2 of Abs that acquire novel antigen-binding specificities after interaction with heme. Tyr is a well known amino acid that can interact with heme. It is found in the heme binding regions of

proteins (34). Tyr can contact heme both by aromatic interactions and by coordination of central iron ion of heme (through its hydroxyl group). Aromatic amino acid residues such as tyrosine, phenylalanine and tryptophan are usually localized in the interior of proteins. But immunoglobulins are unusual in that they carry large number of aromatic amino acids exposed to the protein surface, and more specifically in CDRs (35,36). Thus, presence of Tyr in the antigen-binding site can provide appropriate environment for binding of aromatic compounds such as heme. The observed higher frequency of Tyr in the antigen-binding site corroborates a result from a study where the heme-induced gain in reactivity to gp120 of HIV-1 of human monoclonal Abs, isolated from seronegative individuals, was elucidated (24). Besides Tyr residues, the binding of Abs correlated with elevated numbers of positively charged residues such as Lys and Arg in the CDRs. These residues can interact through ion bonds with carboxyl groups of heme (Fig. 1A), thus further facilitating the bonding of heme to IgG.

Our data revealed that heme can well detect elevated number of positive amino acid residues and aromatic residues in Abs. The capacity of heme to detect both an increased presence of aromatic and positively charged amino acid residues in the V region well explains the strong correlation of certain developability parameters with the binding to heme. Thus, the higher frequency of Tyr in the V regions was associated with an augmented hydrophobicity of the Abs and an increased tendency for homophilic binding (self-association) (37). On the other hand, the higher prevalence of residues with positive charge or patches with positive charge in the antigen-binding site has been demonstrated to correlate with an increased polyreactivity (37-41). These observations imply that the binding to heme can serve as an integral probe that simultaneously evaluates three qualities of antibodies with a high negative impact on developability. The utility of heme as a probe stems from intrinsic properties of this cofactor. Notably, heme is a macrocyclic compound with unique chemical structure (Fig. 1A) that encompasses diverse chemical groups, thus allowing establishment of various types of non-covalent molecular interactions *e.g.* hydrophobic, van der Waals, π-stacking, hydrogen and ion bonding, as well as metal coordination.

Since the heme-binding assay used in the present study is simple and allows high-throughput screening in a short time, large number of Abs can be assessed, thus saving time and resources associated with the employment of multiple complex developability assays. The feasibility of binding to heme as an analytical tool for detection of Ab liabilities was also suggested by the fact that only 18 % of top heme-binding Abs has been approved for clinical practice, whereas 41 % of Abs were approved among therapeutic Abs with lower or no heme binding capacity.

Assessment of heme-induced polyreactivity provides a novel dimension for analyses of Ab developability. The cryptic polyreactivity can be of relevance in multiple disease conditions associated with hemolysis and tissue damage, where extracellular heme is available. Thus, it is very probable that some of the patients treated with monoclonal Abs for cancer or autoimmunity could experience release of heme and thus present with an environment that would compromise the efficacy of therapeutic Ab with an inherent potential to acquire polyreactivity upon contact with heme. In conclusion, our study strongly suggests that binding to immobilized heme and heme-mediated induction of Ab polyreactivity have capacity to predict several negative characteristics of Ab that can compromise their introduction into the clinical practice.

Experimental procedures

Antibodies

In the present study, we used 113 samples with variable region sequences corresponding to therapeutic antibodies that are approved for use in clinic or preceded as far as Phase II and Phase III clinical trials, with vesencumab being the lone exception. All antibodies were expressed as human IgG1 in HEK293 cells. A detailed description of production of this set of recombinant antibodies was provided in Jain et al (17). All reagents used in the study were with the highest purity available.

Antibody reactivity to surface immobilized heme

For covalent in situ immobilization of heme or folic acid through their carboxyl groups, we applied amino-coupling procedure previously described in (42). In brief, 96-well polystyrene plates NUNC MaxiSorp™ (Thermo Fisher Scientific, Waltham, MA) were incubated for 1 hour at RT with 100 µl/well of solution in PBS of 0.5 % laboratory-grade gelatin (J.T. Baker Chemicals, Fisher Scientific). After 3 washes with deionized water, 50 µl/well of 1 mM solution of hemin (Fe(III)-protoporphyrin IX chloride, Frontier Scientific, Inc., Logan, UT) or alternatively - folic acid (FA, Sigma-Aldrich, St. Louis, MO) were added. Both substances were diluted in 1:1 DMSO:water mixture. To wells containing hemin, FA or vehicle only, 25 µl/well of 60 mM water solution of 1-ethyl-3-(3-dimethylaminopropyl) carbodiimide hydrochloride (EDC, Thermo Fisher Scientific) were added, resulting in final concentration of 20 mM. The conjugation reaction between activated carboxyl groups of heterocyclic compounds and amino groups from gelatin was left to occur for 2 hours at RT, in dark, with periodic gentle shaking of the plates. After, the plates were washed 3 times with deionized water. To inactivate EDC-activated carboxyl groups on gelatin, all wells were incubated for 5 min with 100 µl/well of excess (1M solution) of ethanolamine, pH 8, and then washed thoroughly with deionized water. Next, plates were incubated for 1 hour with PBS containing 0.25 % Tween 20. All analyzed recombinant IgG1 antibodies were diluted to 20 µg/ml in PBS containing 0.05 % Tween 20 (PBS-T) and incubated for 1 hour at RT with surface immobilized heme (or FA). As a control, each antibody was also incubated with wells coated with gelatin only. The plates contained also a standard, which represented 100 µg/ml of pooled human IgG (IVIg, Endobulin, Baxter, USA) incubated with surface immobilized heme (or FA). In another experimental setting, selected antibodies demonstrating the highest heme-binding activity were analyses at serial (3 × each step) dilutions starting from concentration of 30 µg/ml (200 nM). After incubation with antibodies, the plates were washed at least 5 times with PBS-T and then incubated for 1 hour at RT with HRP-conjugated anti-human IgG (Fc-specific, clone JDC-10, Southern Biotech, Birmingham, AL) diluted 3000 × in PBS-T. Following washing with PBS-T, the immunoreactivity of the antibodies was revealed by addition of peroxidase substrate, *o*-phenylenediamine dihydrochloride (Sigma-Adrich). The measurement of the optical density at 492 nm was performed after addition of 2M HCl with a microplate reader (Infinite 200 Pro, Tecan, Männedorf, Switzerland).

Real time analyses of interaction of heme with antibodies

Surface plasmon resonance (SPR)-based assay (Biacore 2000, Biacore GE Healthcare, Uppsala, Sweden) was applied to elucidate kinetics of interaction of heme with therapeutic antibodies. Antibodies demonstrating substantial binding to immobilized heme - figitumumab, fulranumab and tigatuzumab were covalently coupled to surface of CM5 sensor chips (Biacore) using amino-coupling kit (Biacore). In brief, the antibodies were diluted in 5 mM maleic acid solution, pH 4 to final concentration of 20 µg/ml and injected for 7 min over sensor surfaces pre-activated by a mixture of EDC / N-hydroxysuccinimide. Unconjugated carboxyl groups were saturated by injection of 1M solution of ethanolamine.HCl. All measurements were performed using HBS-EP buffer with following composition: 10 mM HEPES pH 7.2; 150 mM NaCl; 3 mM EDTA, and 0.005 % Tween 20. The binding analyses were performed at temperature of 25 °C. Hemin (1 mM stock solution in 0.05 NaOH) was always sequentially diluted in HBS-EP to concentrations of 1250, 625, 312.5, 156.25, 78.1, 39 and 19.5 nM. For each concentration, the dilution sequence was repeated immediately before injection. The buffer flow rate during all real-time interaction measurements was set at 30 µl/min. The association and dissociation phases of the binding of hemin to the immobilized antibodies were monitored for 5 min. The binding of hemin to reference channel containing activated and deactivated carboxymethylated dextran only was used as negative control and was subtracted from the binding during data processing. The sensor chip surfaces were regenerated by 30 sec exposure to a solution 3M solution of KSCN (Sigma-Aldrich). The assessment of binding kinetics was performed by BIAevaluation version

4.1.1 Software (Biacore) by using Langmuir binding model.

Analysis of polyreactivity of therapeutic antibodies following exposure to heme

1. ELISA

Ninety-six-well polystyrene plates NUNC MaxiSorp™ (Thermo Fisher Scientific) were coated for one hour at RT with human recombinant factor VIII (Advate, Baxter), human plasma-derived C3 (CompTech, Tyler, TX) and recombinant LysM polypeptide of AtlA from *Enterococcus faecalis* (kindly provided by Dr. Stephan Mesnage, University of Sheffield, UK). All proteins were diluted to 3 µg/ml in PBS. After blocking by incubation for one hour with 0.25 % solution of Tween 20 in PBS, the plates were incubated with therapeutic antibodies. Each antibody was first diluted in PBS to 100 µg/ml, exposed or not for 10 min to 5 µM of hemin (stock solution in DMSO) and then diluted to 20 µg/ml in PBS-T and incubated with coated proteins for 90 min at RT. As an internal control each plate was incubated with 250 µg/ml of native pooled human IgG. For assessment of binding of each recombinant antibody in native and heme-exposed form to the studied proteins, the plates were first washed 5 times with PBS-T and then incubated for 1 hour at RT with HRP-conjugated anti-human IgG (Fc-specific, clone JDC-10, Southern Biotech, Birmingham, AL) diluted 3000 × in PBS-T. Following washing with PBS-T, the immunoreactivity of the antibodies was revealed by addition of peroxidase substrate, *o*-phenylenediamine dihydrochloride (Sigma-Adrich). The measurement of the optical density at 492 nm was performed after addition of 2M HCl with a microplate reader (Infinite 200 Pro, Tecan, Männedorf, Switzerland).

2. Immunoblot

Lysate of *Bacillus anthracis* was loaded on a 4-12 % gradient NuPAGE Novex SDS-PAGE gel (Invitrogen, Thermo Fisher). After migration, proteins were transferred on nitrocellulose membranes (iBlot gel transfer stacks, Invitrogen, Thermo Fisher) by using iBlot electrotransfer system (Invitrogen, Thermo Fisher). Membranes were blocked overnight at 4 °C in PBS buffer containing Tween 0.1% (PBS-T). Next, the membranes were fixed on Miniblot system (Immunetics, Cambridge, MA) and incubated for 2 hours at RT with 10 µg/ml of selected native or heme-exposed therapeutic antibodies. The antibodies were pre-treated at 50 µg/ml in PBS with 5 µM hemin for 10 min and diluted in PBS-T before loading. Membranes were washed (6 × 10 min) with excess of PBS-T before being incubated for one hour at RT with an alkaline phosphatase-conjugated goat anti-human IgG (Southern Biotech, Birmingham, AL), diluted 3000 × in PBS-T. Membranes were then thoroughly washed (6 × 10 min) with PBS-T before revealed with SigmaFast NBT/BCIP substrate solution (Sigma-Aldrich).

Real time analyses of interaction of antibodies with human FcRn

The binding of selected heme-sensitive antibodies to human FcRn before and after exposure to heme was studied by SPR-based biosensor technology (Biacore). Biotinylated recombinant human FcRn (Amsbio LLC, Cambridge, MA) was diluted to 5 µg/ml in running buffer - 100 mM Tris pH 6 (adjusted by addition of dry citric acid), 100 mM NaCl, 5 % Glycerol and 0.1% Tween 20 - and injected with flow rate of 10 µl/min over the pre-activated sensor chip surface, coated with streptavidin by manufacturer (SA chip, Biacore). We aimed to achieve approximately 0.5 ng/mm^2 immobilization density on the sensor surface. For kinetics analyses, the therapeutic antibodies figitumumab, fulranumab and teplizumab were first diluted in PBS to 100 µg/ml (670 nM) and treated with 6.7 µM of hemin (1 mM stock solution in DMSO) or with vehicle only. Following 5 min incubation on ice, the native and heme-exposed antibodies were serially diluted in the binding buffer to following concentrations - 25, 12.5, 6.25, 3.125, 1.56, 0.78, 0.39 and 0.195 nM. The interaction with surface immobilized FcRn was performed at flow rate of 30 µl/min. The association and dissociation phases of the binding of antibodies at different concentrations to the immobilized FcRn were monitored for 4 and 5 min, respectively. For regeneration of the binding surface, the chip was exposed for 30 sec to a solution 100 mM TRIS pH

7.7/ 100 mM NaCl and this step was repeated twice for the highest concentration of samples (25 and 12.5 nM). The analysis was performed at 25 °C. The assessment of binding kinetics was done by BIAevaluation version 4.1.1 Software (Biacore) by using global kinetics analyses and Langmuir binding model.

Absorbance spectroscopy

We used high-throughput absorbance spectroscopy to elucidate the interaction of the repertoire of therapeutic antibodies with hemin in solution. The recombinant antibodies were first diluted to 200 µg/ml in PBS. The dilutions were performed directly in UV-star 96-well microplates (Greiner Bio-One, Les Ulis, France). To 100 µl of antibody solution, equal volume of freshly prepared hemin solution (10 µM in PBS) was added and intensively homogenized. Resulting concentration of antibodies was 100 µg/ml (670 nM) and of heme was 5 µM. As control heme was added to buffer only. The plates were incubated for 30 min at RT in dark. The absorbance spectra in the wavelength range between 350 – 450 nm were recorded by using Tecan Infinite 200 Pro, microplate reader. The spectral resolution was 2 nm. All measurements were done at RT. To assess the changes in spectral properties of heme upon interaction with antibodies, the shift in maximal absorbance wavelength was defined as follows: λ-shift = λ_{max} of hemin alone – λ_{max} of hemin in the presence of antibody. The differential spectra (absorbance spectrum of hemin in the presence of antibody – absorbance spectrum of hemin alone) allowed quantification of the maximal increase in the absorbance intensity (ΔA).

Peroxidase assay

To evaluate how interaction with antibodies influences the intrinsic peroxidase activity of heme, we performed colorimetric catalytic assay. The antibodies from the studied repertoire were first diluted in PBS to 100 µg/ml (670 nM) and exposed to 5 µM final concentration of hemin. Following 90 min incubation at RT, 50 µl of antibody exposed to hemin or hemin in PBS only were mixed with 150 µl of reaction buffer (0.15 M citrate-phosphate buffer pH 5) containing 0.9 mM of 2,2-Azino-bis(3-ethylbenzothiazoline-6-sulfonic acid) diammonium salt (ABTS, Sigma-Aldrich) and 6 mM H_2O_2. The reaction was performed in 96 well microtiter plates at RT in dark. The absorbance at 414 nM was recorded at 10 and 20 min after mixing by using Tecan Infinite 200 Pro, microplate reader. The peroxidase activity of BSA at 150 µg/ml exposed to 5 µM hemin was used as a control.

Structural modeling of the variable regions of antibodies and molecular docking

For modeling of three dimensional structures of the variable domains of heavy and light chains of selected heme-binding and heme-sensitive antibodies, we used sequence-based modeling algorithm - RosettaAntibody3 program (43-46). The amino acid sequences of the variable regions were loaded to ROSIE online server (http://antibody.graylab.jhu.edu/). Relaxed 3D models with lowest free energy were visualized by using Chimera UCSF Chimera package. Chimera is developed by the Resource for Biocomputing, Visualization, and Informatics at the University of California, San Francisco (supported by NIGMS P41-GM103311) (47). Chimera software was also used for visualization of Coulombic electrostatic potential of antigen-binding sites as well as to highlight the surface exposed Tyr residues in the antigen-binding site.

The structural model of antibody variable region of tigatuzumab was used as an input for docking of protoporphyrin IX. To this end, we used SwissDock web service, which uses CHARM force field and it is dedicated to the prediction of protein-small molecule interaction (48,49). The three-dimensional structures of the most probable complex were visualized by using Chimera software.

Statistical analyses

Abs that meet the following criteria were included in statistical analyses: availability of sequence information (obtained from IMGT/mAb-DB database (http://www.imgt.org/mAb-DB/) or from the article of Jain et al. (17), availability of the interaction parameters obtained in the present study and availability of data about biophysical measurements performed in the study of Jain (17). Estimation of the composition and length of CDR regions as well as number of amino acid

replacements in V domains was performed by IMGT/JunctionAnalysis tool (50,51).

The antibody binding intensity to immobilized heme and FA, average degree of antibody binding to protein antigens (FVIII, C3 and LysM) after heme exposure, increase in absorbance intensity and the wavelength number shift in maximal absorbance at Soret band as well as fold increase in the catalytic activity of complexes of heme with antibodies as compared to heme also were used as input for correlation analyses. Thus experimental measurable of therapeutic Abs were correlated with different features of variable regions – number of somatic mutations in V_H and V_L domains, lengths of CDRH3, CDRH2 and CDRL3, number of charged, polar, aromatic, and hydrophobic residues in the CDR regions, and frequency of individual amino acid residues in CDR regions. Correlation analyses were performed by non-parametric Spearman's rank-order analysis using Graph Pad Prism v.6 software (La Jolla, CA). A significant correlation was considered only if P value ≤ 0.05. Principal component analysis (PCA) was performed on R software (http://www.R-project.org/) with the FactoMineR package (52). As per Jain et al. (17) , values for SGAC100 were negated before applying PCA.

Acknowledgments

All the antibodies characterized in this work were produced, purified, and subjected to quality control through the combined efforts from the molecular core, high throughput expression and protein analytics departments at Adimab LLC. We are grateful to Dr. Max Vásquez, Dr Yingda Xu and Dr Tushar Jain (Adimab, USA) for their vital support and discussions.

Funding information

This work was supported by Institut National de la Santé et de la Recherche Médicale (INSERM, France), Centre National de la Recherche Scientifique (CNRS, France), by the European Research Council (Project CoBABATI ERC-StG-678905 to J.D.D.) and by a grant from "Fondation ARC pour la recherche sur le cancer", France (PJA 20171206410).

Funding information: The authors declare no conflicts of interest in regard to this manuscript

References

1. Kaplon, H., and Reichert, J. M. (2019) Antibodies to watch in 2019. *mAbs* **11**, 219-238
2. Kaplon, H., Muralidharan, M., Schneider, Z., and Reichert, J. M. (2020) Antibodies to watch in 2020. *mAbs* **12**, 1703531
3. Jarasch, A., Koll, H., Regula, J. T., Bader, M., Papadimitriou, A., and Kettenberger, H. (2015) Developability assessment during the selection of novel therapeutic antibodies. *J Pharm Sci* **104**, 1885-1898
4. Dashivets, T., Stracke, J., Dengl, S., Knaupp, A., Pollmann, J., Buchner, J., and Schlothauer, T. (2016) Oxidation in the complementarity-determining regions differentially influences the properties of therapeutic antibodies. *mAbs* **8**, 1525-1535
5. Lu, X., Nobrega, R. P., Lynaugh, H., Jain, T., Barlow, K., Boland, T., Sivasubramanian, A., Vasquez, M., and Xu, Y. (2019) Deamidation and isomerization liability analysis of 131 clinical-stage antibodies. *mAbs* **11**, 45-57
6. Xu, Y., Wang, D., Mason, B., Rossomando, T., Li, N., Liu, D., Cheung, J. K., Xu, W., Raghava, S., Katiyar, A., Nowak, C., Xiang, T., Dong, D. D., Sun, J., Beck, A., and Liu, H. (2019) Structure, heterogeneity and developability assessment of therapeutic antibodies. *mAbs* **11**, 239-264

7. Steinmeyer, D. E., and McCormick, E. L. (2008) The art of antibody process development. *Drug Discov Today* **13**, 613-618
8. Sule, S. V., Sukumar, M., Weiss, W. F. 4th, Marcelino-Cruz, A. M., Sample, T., and Tessier, P. M. (2011) High-throughput analysis of concentration-dependent antibody self-association. *Biophys J* **101**, 1749-1757
9. Hotzel, I., Theil, F. P., Bernstein, L. J., Prabhu, S., Deng, R., Quintana, L., Lutman, J., Sibia, R., Chan, P., Bumbaca, D., Fielder, P., Carter, P. J., and Kelley, R. F. (2012) A strategy for risk mitigation of antibodies with fast clearance. *mAbs* **4**, 753-760
10. Liu, Y., Caffry, I., Wu, J., Geng, S. B., Jain, T., Sun, T., Reid, F., Cao, Y., Estep, P., Yu, Y., Vasquez, M., Tessier, P. M., and Xu, Y. (2014) High-throughput screening for developability during early-stage antibody discovery using self-interaction nanoparticle spectroscopy. *mAbs* **6**, 483-492
11. Sharma, V. K., Patapoff, T. W., Kabakoff, B., Pai, S., Hilario, E., Zhang, B., Li, C., Borisov, O., Kelley, R. F., Chorny, I., Zhou, J. Z., Dill, K. A., and Swartz, T. E. (2014) In silico selection of therapeutic antibodies for development: viscosity, clearance, and chemical stability. *Proc Natl Acad Sci USA* **111**, 18601-18606
12. Kohli, N., Jain, N., Geddie, M. L., Razlog, M., Xu, L., and Lugovskoy, A. A. (2015) A novel screening method to assess developability of antibody-like molecules. *mAbs* **7**, 752-758
13. Kelly, R. L., Sun, T., Jain, T., Caffry, I., Yu, Y., Cao, Y., Lynaugh, H., Brown, M., Vasquez, M., Wittrup, K. D., and Xu, Y. (2015) High throughput cross-interaction measures for human IgG1 antibodies correlate with clearance rates in mice. *mAbs* **7**, 770-777
14. Avery, L. B., Wade, J., Wang, M., Tam, A., King, A., Piche-Nicholas, N., Kavosi, M. S., Penn, S., Cirelli, D., Kurz, J. C., Zhang, M., Cunningham, O., Jones, R., Fennell, B. J., McDonnell, B., Sakorafas, P., Apgar, J., Finlay, W. J., Lin, L., Bloom, L., and O'Hara, D. M. (2018) Establishing in vitro in vivo correlations to screen monoclonal antibodies for physicochemical properties related to favorable human pharmacokinetics. *mAbs* **10**, 244-255
15. van der Kant, R., Karow-Zwick, A. R., Van Durme, J., Blech, M., Gallardo, R., Seeliger, D., Assfalg, K., Baatsen, P., Compernolle, G., Gils, A., Studts, J. M., Schulz, P., Garidel, P., Schymkowitz, J., and Rousseau, F. (2017) Prediction and Reduction of the Aggregation of Monoclonal Antibodies. *J Mol Biol* **429**, 1244-1261
16. Kraft, T. E., Richter, W. F., Emrich, T., Knaupp, A., Schuster, M., Wolfert, A., and Kettenberger, H. (2020) Heparin chromatography as an in vitro predictor for antibody clearance rate through pinocytosis. *mAbs* **12**, 1683432
17. Jain, T., Sun, T., Durand, S., Hall, A., Houston, N. R., Nett, J. H., Sharkey, B., Bobrowicz, B., Caffry, I., Yu, Y., Cao, Y., Lynaugh, H., Brown, M., Baruah, H., Gray, L. T., Krauland, E. M., Xu, Y., Vasquez, M., and Wittrup, K. D. (2017) Biophysical properties of the clinical-stage antibody landscape. *Proc Natl Acad Sci USA* **114**, 944-949
18. Dimitrov, J. D., Planchais, C., Roumenina, L. T., Vassilev, T. L., Kaveri, S. V., and Lacroix-Desmazes, S. (2013) Antibody polyreactivity in health and disease: statu variabilis. *J Immunol* **191**, 993-999
19. Shehata, L., Maurer, D. P., Wec, A. Z., Lilov, A., Champney, E., Sun, T., Archambault, K., Burnina, I., Lynaugh, H., Zhi, X., Xu, Y., and Walker, L. M. (2019) Affinity Maturation Enhances Antibody Specificity but Compromises Conformational Stability. *Cell Rep* **28**, 3300-3308 e3304
20. McIntyre, J. A., Wagenknecht, D. R., and Faulk, W. P. (2005) Autoantibodies unmasked by redox reactions. *J Autoimmun* **24**, 311-317
21. Dimitrov, J. D., Roumenina, L. T., Doltchinkova, V. R., Mihaylova, N. M., Lacroix-Desmazes, S., Kaveri, S. V., and Vassilev, T. L. (2007) Antibodies use heme as a cofactor to extend their pathogen elimination activity and to acquire new effector functions. *J Biol Chem* **282**, 26696-26706

22. Mihaylova, N. M., Dimitrov, J. D., Djoumerska-Alexieva, I. K., and Vassilev, T. L. (2008) Inflammation-induced enhancement of IgG immunoreactivity. *Inflamm Res* **57**, 1-3
23. McIntyre, J. A., and Faulk, W. P. (2009) Redox-reactive autoantibodies: biochemistry, characterization, and specificities. *Clin Rev Allergy Immunol* **37**, 49-54
24. Lecerf, M., Scheel, T., Pashov, A. D., Jarossay, A., Ohayon, D., Planchais, C., Mesnage, S., Berek, C., Kaveri, S. V., Lacroix-Desmazes, S., and Dimitrov, J. D. (2015) Prevalence and gene characteristics of antibodies with cofactor-induced HIV-1 specificity. *J Biol Chem* **290**, 5203-5213
25. McIntyre, J. A., and Faulk, A. W. (2010) Autoantibody potential of cancer therapeutic monoclonal antibodies. *Intl J Cancer* **127**, 491-496
26. Roumenina, L. T., Rayes, J., Lacroix-Desmazes, S., and Dimitrov, J. D. (2016) Heme: Modulator of Plasma Systems in Hemolytic Diseases. *Trends Mol Med* **22**, 200-213
27. Robin, G., Sato, Y., Desplancq, D., Rochel, N., Weiss, E., and Martineau, P. (2014) Restricted diversity of antigen binding residues of antibodies revealed by computational alanine scanning of 227 antibody-antigen complexes. *J Mol Biol* **426**, 3729-3743
28. McIntyre, J. A., Wagenknecht, D. R., and Faulk, W. P. (2006) Redox-reactive autoantibodies: detection and physiological relevance. *Autoimmun Rev* **5**, 76-83
29. Gupta, N., de Wispelaere, M., Lecerf, M., Kalia, M., Scheel, T., Vrati, S., Berek, C., Kaveri, S. V., Despres, P., Lacroix-Desmazes, S., and Dimitrov, J. D. (2015) Neutralization of Japanese Encephalitis Virus by heme-induced broadly reactive human monoclonal antibody. *Sci Rep* **5**, 16248
30. Pavlovic, S., Zdravkovic, N., Dimitrov, J. D., Djukic, A., Arsenijevic, N., Vassilev, T. L., and Lukic, M. L. (2011) Intravenous immunoglobulins exposed to heme (heme IVIG) are more efficient than IVIG in attenuating autoimmune diabetes. *Clin Immunol* **138**, 162-171
31. Djoumerska-Alexieva, I., Roumenina, L. T., Stefanova, T., Vassilev, T., and Dimitrov, J. D. (2017) Heme-Exposed Pooled Therapeutic IgG Improves Endotoxemia Survival. *Inflammation* **40**, 117-122
32. Xu, Y., Roach, W., Sun, T., Jain, T., Prinz, B., Yu, T. Y., Torrey, J., Thomas, J., Bobrowicz, P., Vasquez, M., Wittrup, K. D., and Krauland, E. (2013) Addressing polyspecificity of antibodies selected from an in vitro yeast presentation system: a FACS-based, high-throughput selection and analytical tool. *Protein Eng Des Sel* **26**, 663-670
33. Kanyavuz, A., Marey-Jarossay, A., Lacroix-Desmazes, S., and Dimitrov, J. D. (2019) Breaking the law: unconventional strategies for antibody diversification. *Nat Rev Immunol* **19**, 355-368
34. Brewitz, H. H., Goradia, N., Schubert, E., Galler, K., Kuhl, T., Syllwasschy, B., Popp, J., Neugebauer, U., Hagelueken, G., Schiemann, O., Ohlenschlager, O., and Imhof, D. (2016) Heme interacts with histidine- and tyrosine-based protein motifs and inhibits enzymatic activity of chloramphenicol acetyltransferase from Escherichia coli. *Biochim Biophys Acta* **1860**, 1343-1353
35. Sundberg, E. J., and Mariuzza, R. A. (2002) Molecular recognition in antibody-antigen complexes. *Adv Protein Chem* **61**, 119-160
36. Wang, M., Zhu, D., Zhu, J., Nussinov, R., and Ma, B. (2018) Local and global anatomy of antibody-protein antigen recognition. *J Mol Recognit* **31**, e2693
37. Lecerf, M., Kanyavuz, A., Lacroix-Desmazes, S., and Dimitrov, J. D. (2019) Sequence features of variable region determining physicochemical properties and polyreactivity of therapeutic antibodies. *Mol Immunol* **112**, 338-346
38. Birtalan, S., Zhang, Y., Fellouse, F. A., Shao, L., Schaefer, G., and Sidhu, S. S. (2008) The intrinsic contributions of tyrosine, serine, glycine and arginine to the affinity and specificity of antibodies. *J Mol Biol* **377**, 1518-1528
39. Kelly, R. L., Zhao, J., Le, D., and Wittrup, K. D. (2017) Nonspecificity in a nonimmune human scFv repertoire. *mAbs* **9**, 1029-1035

40. Rabia, L. A., Zhang, Y., Ludwig, S. D., Julian, M. C., and Tessier, P. M. (2018) Net charge of antibody complementarity-determining regions is a key predictor of specificity. *Protein Eng Des Sel* **31**, 409-418
41. Raybould, M. I. J., Marks, C., Krawczyk, K., Taddese, B., Nowak, J., Lewis, A. P., Bujotzek, A., Shi, J., and Deane, C. M. (2019) Five computational developability guidelines for therapeutic antibody profiling. *Proc Natl Acad Sci USA* **116**, 4025-4030
42. Bozinovic, N., Noe, R., Kanyavuz, A., Lecerf, M., and Dimitrov, J. D. (2020) Method for identification of heme-binding proteins and quantification of their interactions. *Anal Biochem*, doi: 10.1016/j.ab.2020.113865
43. Marze, N. A., Lyskov, S., and Gray, J. J. (2016) Improved prediction of antibody VL-VH orientation. *Protin Eng Des Sel* **29**, 409-418
44. Sivasubramanian, A., Sircar, A., Chaudhury, S., and Gray, J. J. (2009) Toward high-resolution homology modeling of antibody Fv regions and application to antibody-antigen docking. *Proteins* **74**, 497-514
45. Weitzner, B. D., and Gray, J. J. (2017) Accurate Structure Prediction of CDR H3 Loops Enabled by a Novel Structure-Based C-Terminal Constraint. *J Immunol* **198**, 505-515
46. Weitzner, B. D., Jeliazkov, J. R., Lyskov, S., Marze, N., Kuroda, D., Frick, R., Adolf-Bryfogle, J., Biswas, N., Dunbrack, R. L., Jr., and Gray, J. J. (2017) Modeling and docking of antibody structures with Rosetta. *Nat Protoc* **12**, 401-416
47. Pettersen, E. F., Goddard, T. D., Huang, C. C., Couch, G. S., Greenblatt, D. M., Meng, E. C., and Ferrin, T. E. (2004) UCSF Chimera--a visualization system for exploratory research and analysis. *J Comput Chem* **25**, 1605-1612
48. Grosdidier, A., Zoete, V., and Michielin, O. (2011) Fast docking using the CHARMM force field with EADock DSS. *J Comput Chem* **32**, 2149-2159
49. Grosdidier, A., Zoete, V., and Michielin, O. (2011) SwissDock, a protein-small molecule docking web service based on EADock DSS. *Nucleic Acids Res* **39**, W270-277
50. Yousfi Monod, M., Giudicelli, V., Chaume, D., and Lefranc, M. P. (2004) IMGT/JunctionAnalysis: the first tool for the analysis of the immunoglobulin and T cell receptor complex V-J and V-D-J JUNCTIONs. *Bioinformatics* **20 Suppl 1**, i379-385
51. Giudicelli, V., and Lefranc, M. P. (2011) IMGT/junctionanalysis: IMGT standardized analysis of the V-J and V-D-J junctions of the rearranged immunoglobulins (IG) and T cell receptors (TR). *Cold Spring Harbor Protoc* **2011**, 716-725
52. Le, S., Josse, J., and Husson, F. (2007) FactoMineR: An R Package for Multivariate Analysis. *J Stat Soft* **25**, 1-18

Legends to figures

Figure 1. Interaction of heme with therapeutic Abs. (A) Structural formula of Fe(II)protoporphyrin IX (heme). (B) Interaction of the repertoire of monoclonal IgG1 therapeutic antibodies to immobilized heme (left panel) and FA (righ panel). Each circle on the panels represents the average binding intensity of a given therapeutic Ab analysed in duplicate. The binding intensity for each Ab is obtained by division of reactivity to cofactor-conjugated gelatine by the reactivity of Ab to gelatine alone. The dashed line represents the 2-fold increased binding over binding to gelatine alone. The right panel depicts the correlation of the binding to FA versus the binding to heme. The Spearman correlation analyses $\rho = 0.69$, $P < 0.0001$ – indicates significant correlation between the two parameters. The dashed lines display the 95 % confidence band. (C) Concentration-dependent binding of Abs to immobilized heme. The selected 10 Abs were identified as top binders in high-throughput heme-binding assay (panel B). Increasing concentrations 0.09 - 200 nM of the selected Abs were incubated with heme-coated surface or with

control surface. Non-linear regression analyses were performed by Graph Pad Prism v.6 software. (D) Real time interaction profiles of binding of heme to immobilized Abs (figitumumab, fulranumab and tigatuzumab). The black line depicts the binding profiles obtained after injection of serial dilutions of hemin (1250 – 19.5 nM). The red lines depict the fits of data obtained by global analysis using Langmuir kinetic model. (E) The three-dimensional structure of tigatuzumab was modelled by sequence-based variable region modelling algorithm RosettaAntibody implemented on ROSIE web server (http://rosie.rosettacommons.org/). The putative heme-binding site was then predicted by docking of the protoporphyrin IX molecule to the variable region using the SwissDock web service protein-ligand docking platform-based on EADock DSS algorithm (http://www.swissdock.ch/). The figure shows side and top view of the variable region of tigatuzumab. Grey: variable domain of light chain; blue: variable domain of heavy chain. Heme is shown in red.

Figure 2. Binding of heme to Abs in solution. UV-vis absorbance spectroscopy analysis of the interaction of repertoire of therapeutic Abs with hemin. (A) Differential absorbance spectra in the wavelength range 350-450 nm obtained after subtraction of the spectrum of 5 μM hemin in PBS from the spectrum of 5 μM hemin in the presence of 670 nM of monoclonal IgG1. Each line depicts the differential spectrum of an individual Ab. (B) Plot showing the maximal increase of the absorbance intensity of heme in the presence of therapeutic Ab. (C) Plot of the value of the shift of the maximal wavelength in the presence of antibody as compared to the absorbance maxima of heme in PBS only. On panels B and C, each circle depicts the absorbance maximal intensity or shift in the wavelength maxima of individual Ab. (D) Changes of catalytic activity of heme upon interaction with Abs. The oxidation of ABTS was used as colorimetric reaction for assessment of the catalytic activity of heme in absence and presence of monoclonal IgG1. The panel illustrates the fold change in the peroxidase activity, as compared to heme alone in PBS, for repertoire of therapeutic Abs. Each circle depicts the average changes in the peroxidase activity of an individual monoclonal Ab from duplicate readings. The dashed line indicates 2-fold increase in the catalytic activity of heme in the presence of Abs as compared to heme alone.

Figure 3. Heme-induced antigen-binding polyreactivity of Abs. (A) ELISA analysis of the binding of the repertoire of therapeutic Abs to immobilized human (FVIII, C3) and bacterial (LysM AtlA) proteins. Each circle depicts average reactivity of an individual Ab obtained from duplicate samples. The right panels show the global reactivity profile of the repertoire of therapeutic Abs. The protein binding intensity was obtained by dividing the reactivity of given Ab after exposure to heme by the reactivity of the same Ab in its native form. The dashed line represents two-fold increase in the binding. (B) Correlation between reactivities of the therapeutic Abs to different protein antigens upon exposure to heme. Matrix depicts the correlation analyses between reactivity of heme-treated Abs to different proteins and the average reactivity toward the three proteins. The correlation analysis was performed using Spearman's rank-order test. The values of the correlation coefficients (ρ) are shown in the matrix. The red colour in the heat map signifies positive value of correlation coefficient, the blue - negative. The right panel illustrate the statistical significance (P values). (C) Immunoreactivity of selected Abs (top 10 heme-sensitive Abs) towards antigens present in total lysate of *B. anthracis*.

Figure 4. Interaction of heme-binding antibodies with human FcRn. (A) Real-time binding profiles of selected heme-binding and heme-sensitive Abs to surface immobilized human recombinant FcRn. The interaction analyses were performed with native and Abs exposed to excess of hemin. The black lines depict the binding profiles obtained after injection of serial dilutions of monoclonal Abs, native and after heme exposure (25 – 0.195 nM). The red lines depict the fits of data obtained by global analysis using Langmuir kinetic model. All interaction analyses were performed at 25 °C. (B) Values of the kinetic rate constants of association (top panel), dissociation (middle panel) and equilibrium dissociation constant (bottom panel) for binding of native and heme-exposed monoclonal Abs to FcRn. The kinetics data were obtained after analyses of the real-time interaction profiles shown in A.

Figure 5. Correlation between interaction with heme and sequence features of the variable regions of therapeutic Abs. The binding intensity to immobilized cofactors (heme and FA, **Fig. 1B**) and the degree of heme-induced antigen polyreactivity (**Fig. 3A**) were correlated with the sequence characteristics of heavy and light immunoglobulin chain variable regions of the studied therapeutic Abs. The heat map shows the values of the correlation coefficient (ρ) obtained after Spearman's rank-order analysis of the correlation of data from the binding assays with the number of amino acid replacements in heavy chain variable region; the lengths of CDRH3, CDRH2 and CDRL3; or the number of particular amino acid residues that are present in CDRH3, CDRH2 and CDRL3. The red colour in the heat map signifies positive value of correlation coefficient, the blue - negative. The summary of statistical significance (*P* values) is depicted on the right panels.

Figure 6. Molecular features of antigen-binding sites of selected heme binding and heme sensitive Abs. (Left column) Coulomb's electrostatic potential of antigen binding sites of selected Abs. Distribution of the electrostatic charges (blue for positive charge and red for negative charge) was coloured using UCSF Chimera software. The selected polyreactive Abs demonstrated the most pronounced binding to immobilized heme and/or heme-induced polyreactivity. (Right column) Structural models of antigen-binding sites depicting the surface exposed Tyr residues. Grey: variable domain of light chain; blue: variable domain of heavy chain, orange: tyrosine residues. The structural models were visualized by using UCSF Chimera software. All structural models of the variable immunoglobulin regions were built by ROSSIE online server.

Figure 7. Analysis of the correlations among biophysical developability measurables and cofactors interactions parameters. (A) Matrix depicting the correlation of 12 different Ab developability parameters with Ab-binding intensity to immobilized cofactors (heme and FA - binding), the degree of heme-induced antigen polyreactivity (heme-poly), and Ab interaction with heme in solution (λ shift, ΔA and ABTS). The heat map shows the values of correlation coefficient (ρ) obtained after Spearman's rank-order analysis of the correlation of data. The red colour in the heat map signifies positive value of correlation coefficient, the blue - negative. The summary of statistical significance (*P* values) is depicted on the right panel. Data related to the biophysical developability measurables of the antibodies were obtained from the study of Jain et al (17). (B) Graphical output of the Principal Component Analysis where biophysical developability measurables (in black) and cofactors interactions parameters (in green) are represented as vectors in a plane defined by dimension 1 (horizontal axis) and dimension 2 (vertical axis), explaining 25.7 and 15.3% of the variability of the dataset, respectively. Projections of the vectors on each axis account for the quality of representation of the parameters by dimensions 1 and 2. Positively correlated parameters are grouped; negatively correlated parameters are represented in opposite quadrants and non-correlated parameters are shown by orthogonal vectors.

Figure 1

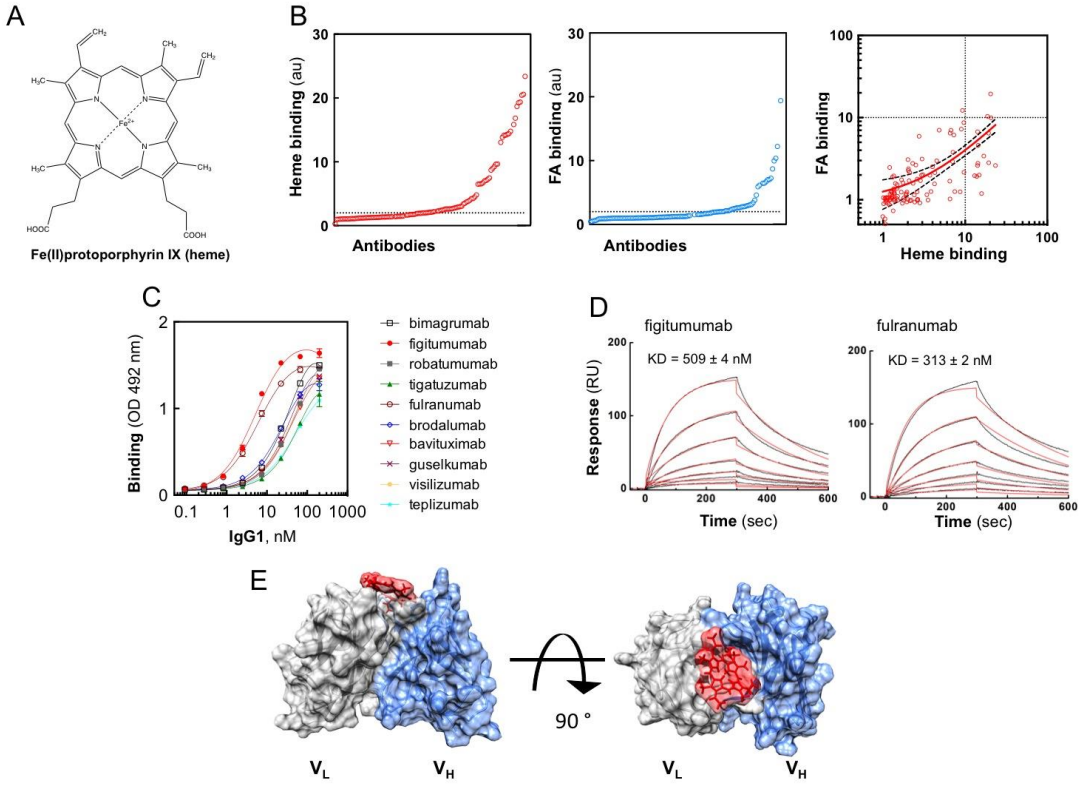
A
Fe(II)protoporphyrin IX (heme)
B
Heme binding (au)
Antibodies
FA binding (au)
Antibodies
FA binding
Heme binding
C
Binding (OD 492 nm)
IgG1, nM
bimagrumab
figitumumab
robatumumab
tigatuzumab
fulranumab
brodalumab
bavituximab
guselkumab
visilizumab
teplizumab
D
figitumumab
KD = 509 ± 4 nM
fulranumab
KD = 313 ± 2 nM
Response (RU)
Time (sec)
E
90 °
VL
VH

Figure 2

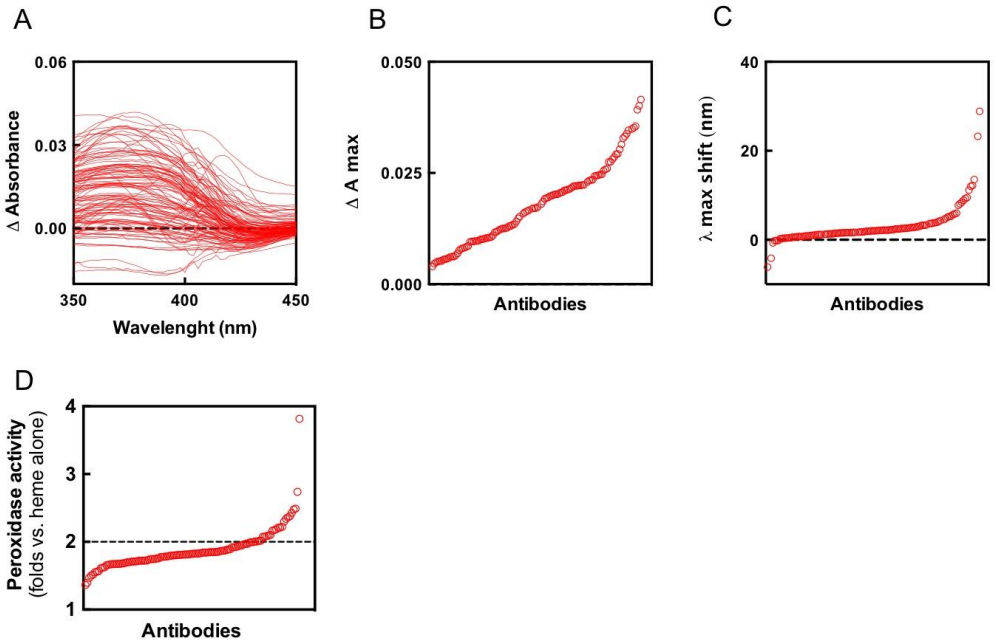
A
0.06
0.03
0.00
Δ Absorbance
350
400
450
Wavelenght (nm)
B
0.050
0.025
0.000
Δ A max
Antibodies
C
40
20
0
λ max shift (nm)
Antibodies
D
4
3
2
1
Peroxidase activity
(folds vs. heme alone)
Antibodies

Figure 3

A

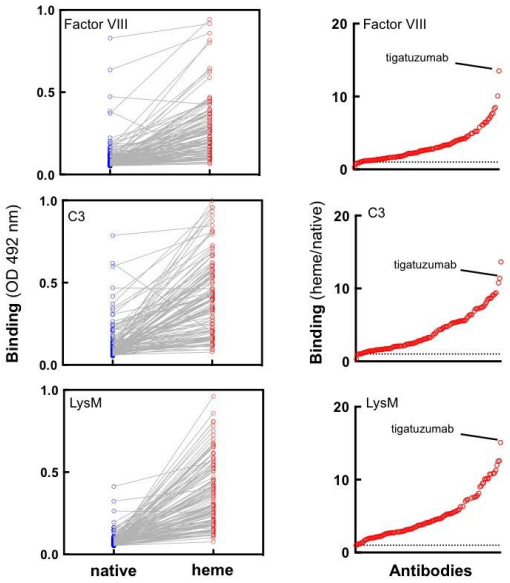
Factor VIII
C3
LysM
Binding (OD 492 nm)
Binding (heme/native)
tigatuzumab
native
heme
Antibodies

B

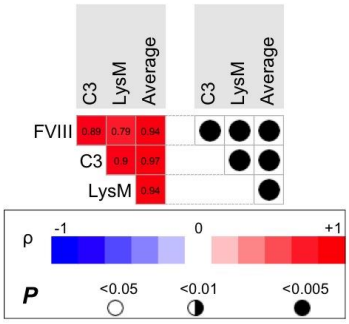
C3
LysM
Average
FVIII
C3
LysM
0.89
0.79
0.94
0.9
0.97
0.94
ρ
-1
0
+1
P
<0.05
<0.01
<0.005

C

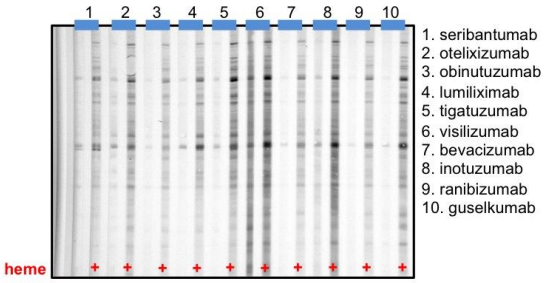
1 2 3 4 5 6 7 8 9 10
1. seribantumab
2. otelixizumab
3. obinutuzumab
4. lumiliximab
5. tigatuzumab
6. visilizumab
7. bevacizumab
8. inotuzumab
9. ranibizumab
10. guselkumab
heme

Figure 4

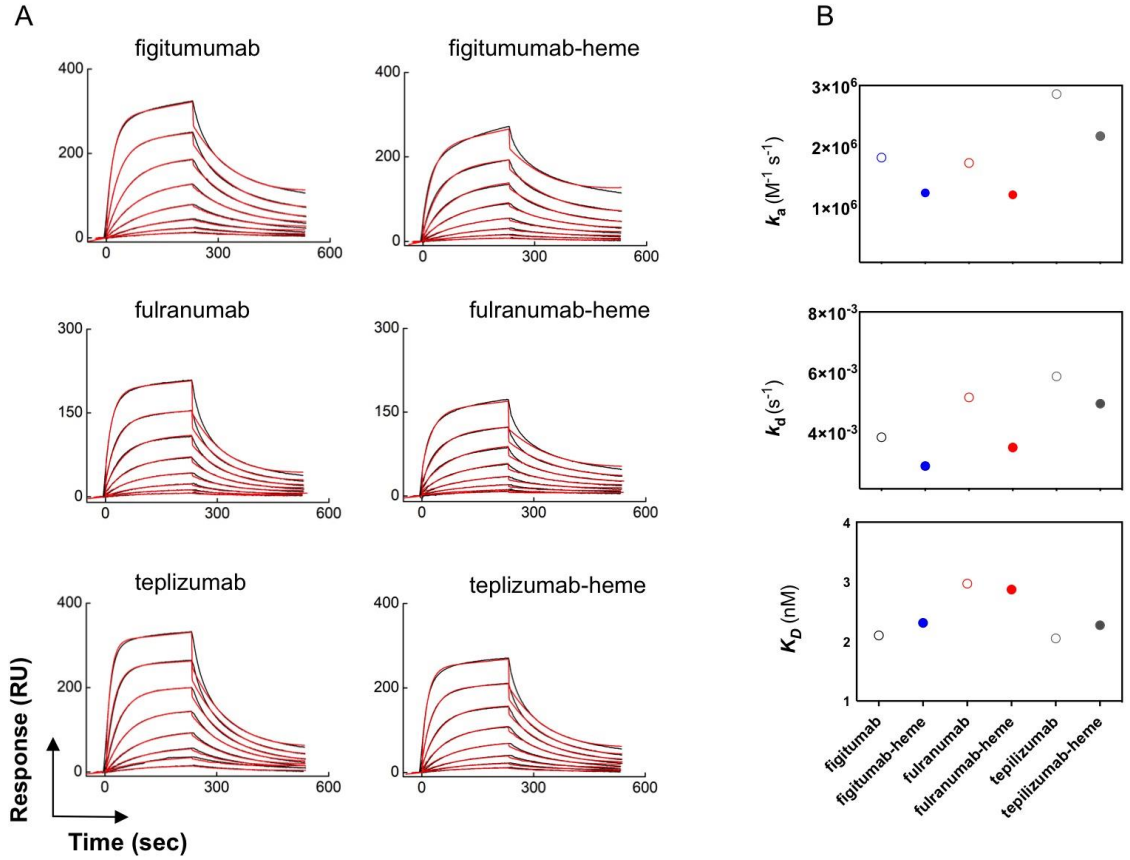
A
figitumumab
figitumumab-heme
fulranumab
fulranumab-heme
teplizumab
teplizumab-heme
Response (RU)
Time (sec)
B
k_a (M^{-1} s^{-1})
k_d (s^{-1})
K_D (nM)
figitumab
figitumab-heme
fulranumab
fulranumab-heme
tepilizumab
tepilizumab-heme

Figure 5

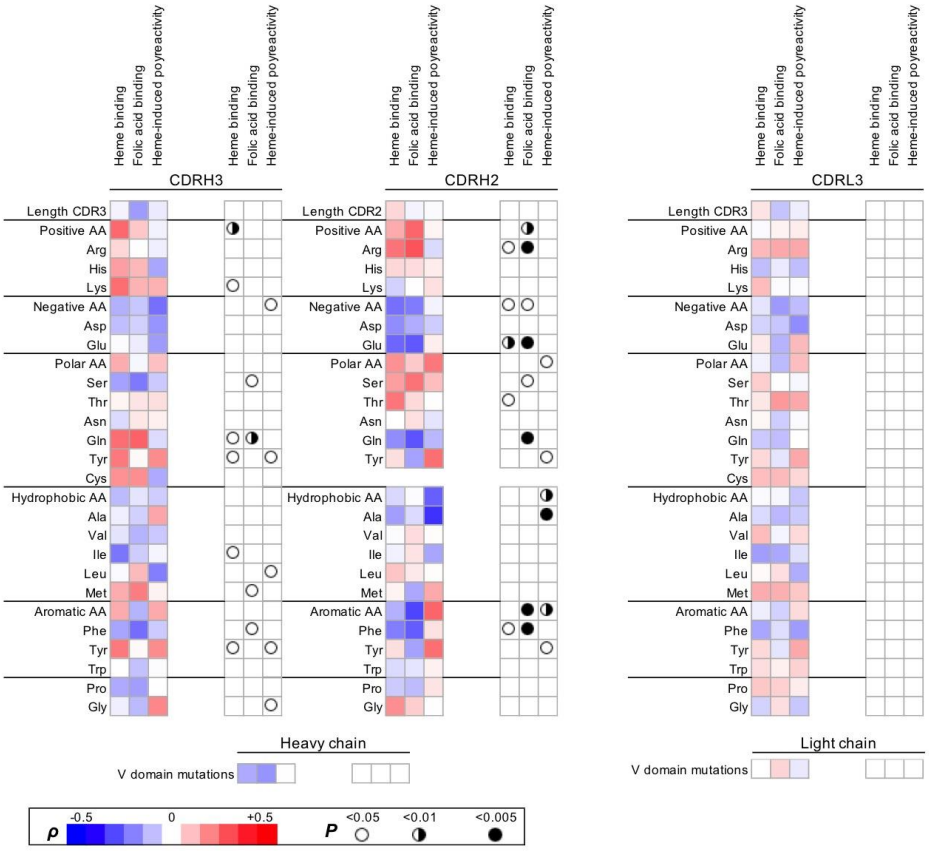
Heme binding
Folic acid binding
Heme-induced poyreactivity
CDRH3
CDRH2
CDRL3
Length CDR3
Length CDR2
Positive AA
Arg
His
Lys
Negative AA
Asp
Glu
Polar AA
Ser
Thr
Asn
Gln
Tyr
Cys
Hydrophobic AA
Ala
Val
Ile
Leu
Met
Aromatic AA
Phe
Tyr
Trp
Pro
Gly
Heavy chain
Light chain
V domain mutations
-0.5
0
+0.5
ρ
P
<0.05
<0.01
<0.005

Figure 6

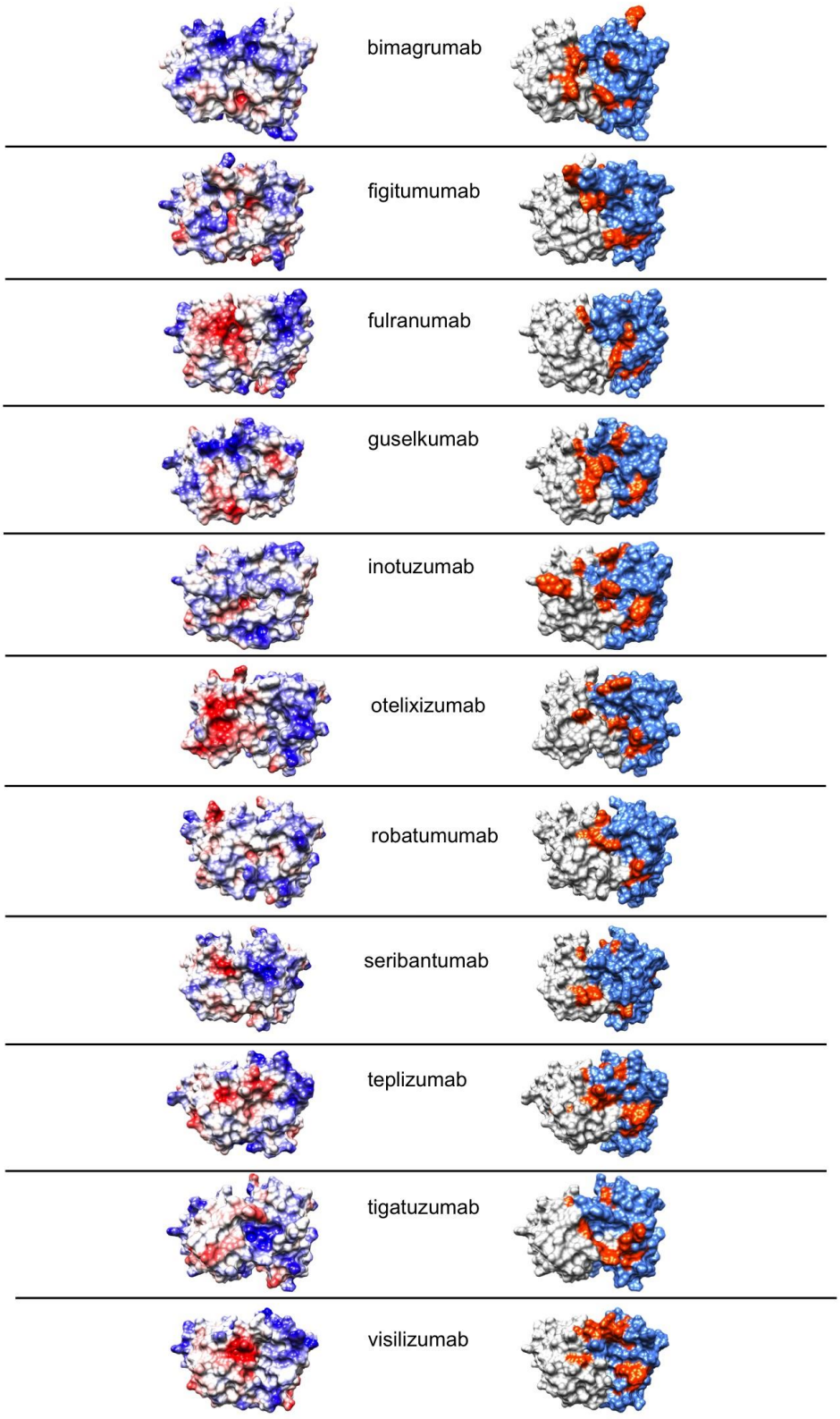
bimagrumab
figitumumab
fulranumab
guselkumab
inotuzumab
otelixizumab
robatumumab
seribantumab
teplizumab
tigatuzumab
visilizumab

Figure 7

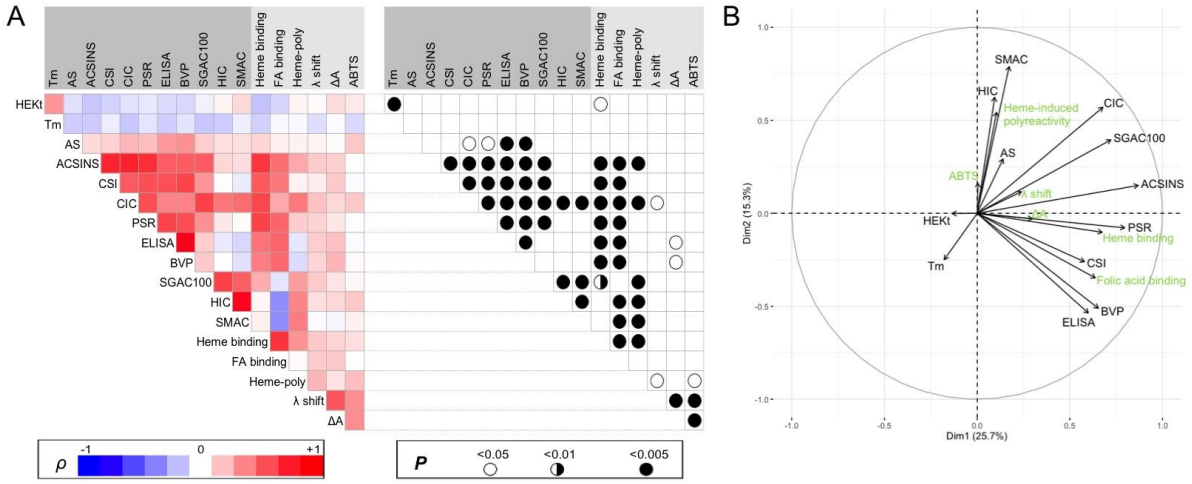
A
Tm
AS
ACSINS
CSI
CIC
PSR
ELISA
BVP
SGAC100
HIC
SMAC
Heme binding
FA binding
Heme-poly
λ shift
ΔA
ABTS
HEKt
ρ
-1
0
+1
P
<0.05
<0.01
<0.005
B
Dim1 (25.7%)
Dim2 (15.3%)
Heme-induced polyreactivity
Folic acid binding